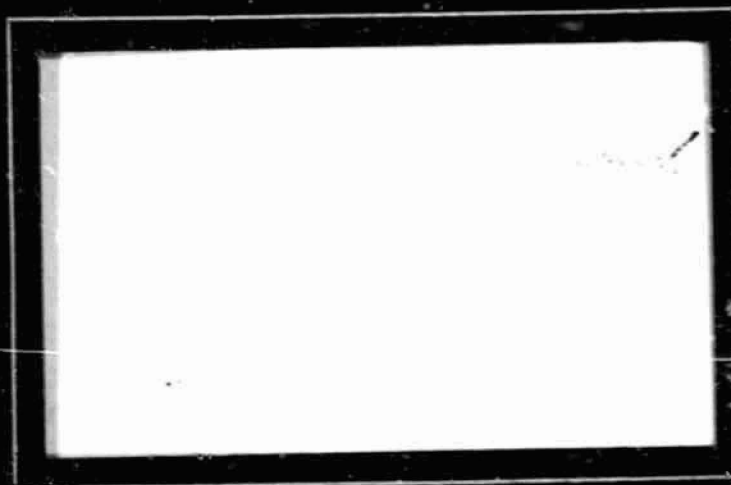


(NASA-CR-136071) BINARY CHROMATOGRAPHIC
DATA AND ESTIMATION OF ADSORBENT
POROSITIES (Rensselaer Polytechnic Inst.)
60 P HC \$5.00 CSCL 07D

N74-10988

H2/06
Unclass
15490



Rensselaer Polytechnic Institute

Troy, New York 12181

R.P.I. Technical Report MP-31

BINARY CHROMATOGRAPHIC DATA AND
ESTIMATION OF ADSORBENT POROSITIES

by

Arthur J. Weisch

National Aeronautics and Space
Administration

Grant NGL 33-018-091

July 1972

School of Engineering
Rensselaer Polytechnic Institute
Troy, New York

ABSTRACT

Data for the system n-pentane/z-heptane on porous Chromosorb-102 adsorbent were obtained at 150, 175, and 200° C for mixtures containing zero to 100% n-pentane by weight. Prior results showing limitations on superposition of pure component data to predict multicomponent chromatograms were verified. The thermodynamic parameter $\ln R_0$ was found to be a linear function of sample composition. A nonporous adsorbent failed to separate the system because of large input sample dispersions. A proposed automated data processing scheme involving magnetic tape recording of the detector signals and processing by a minicomputer was rejected because of resolution limitations of the available A/D converters. Preliminary data on porosity and pore size distributions of the adsorbents were obtained.

PRECEDING PAGE BLANK NOT FILMED

CONTENTS

	Page
ABSTRACT	iii
LIST OF TABLES	v
LIST OF FIGURES	vi
I. INTRODUCTION	1
II. SUMMARY	3
III. BACKGROUND	4
IV. RESULTS AND DISCUSSION	7
A. SUPERPOSITION AND BINARY DATA	7
B. TEMPERATURE EFFECTS	17
C. PRESSURE DEPENDENCE OF mR_0	18
D. DATA ON NON-POROUS PACKING	24
E. SOURCES OF ERROR	33
F. PACKING CHARACTERISTICS	34
G. AUTOMATED DATA PROCESSING	41
V. CONCLUSIONS AND RECOMMENDATIONS	47
VI. ACKNOWLEDGEMENT	49
VII. NOMENCLATURE	50
VIII. REFERENCES	52
IX. APPENDICES	53

LIST OF TABLES

	Page
Table I. Column Characteristics	8
Table II. Experimental Conditions for Binary Data on C-102	9
Table III. Time Lags in Binary Data	11
Table IV. Experimental Conditions for Data on C-1500	25
Table V. Parameter Values for Moment Analysis	29
Table VI. Activation Energies	31
Table VII. Properties of XAD-2	36
Table VIII. Voltage Output from Wheatstone Bridge	45

LIST OF FIGURES

		Page
Figure 1	Predicted and Actual Binary Chromatograms for Pentane-Heptane System on C-102 at 175°C	10
Figure 2	Effect of Composition on Heptane mR_o for Pentane-Heptane System on C-102	12
Figure 3	Effect of Composition on Pentane mR_o for Pentane-Heptane System on C-102	13
Figure 4	Effect of Composition on Heptane mR_o for Pentane-Heptane System (Data of Keba)	15
Figure 5	Effect of Composition on Pentane mR_o for Pentane-Heptane System on C-102 (Data of Keba)	16
Figure 6	Effect of Temperature on Parameter mR_o for C-102	19
Figure 7	Predicted and Actual Chromatograms for Pentane on C-102 at 150°C	20
Figure 8	Predicted and Actual Chromatograms for Heptane on C-102 at 150°C	21
Figure 9	Predicted and Actual Chromatograms for Heptane on C-102 at 175°C	22
Figure 10	Predicted and Actual Chromatograms for Heptane on C-102 at 200°C	23
Figure 11	Predicted and Actual Chromatograms for Heptane on C-1500 at 100°C	26
Figure 12	Predicted and Actual Chromatograms for Heptane on C-1500 at 150°C	27
Figure 13	Prediction of Pentane and Heptane Chromatograms for a Binary Mixture Using Moment Analysis	30
Figure 14	Effect of Temperature on Parameter mR_o for C-1500	32
Figure 15	Structure of v^1D-2	35

	Page
Figure 16 Porosimeter Results for XAD-2	38
Figure 17 Porosimeter Results for C-102	39
Figure 18 Data Processing	42
Figure 19 Detector Control Circuit	44

PART I

INTRODUCTION

The work done for this report is part of a long term effort at Remsselaer (1,2,3,4,5,6) to develop fundamental design techniques for a gas chromatograph. Specifically, the overall project is to develop methods for designing and optimizing a gas chromatograph-mass spectrometer system for use in chemical analysis to be carried out in an unmanned roving vehicle on the surface of Mars, although the results are by no means limited to this application.

A gas chromatograph is a chemical separation device which utilizes the phenomena of adsorption-desorption. Chemical species, carried by an inert or carrier gas, successively adsorb on and desorb from a packed bed of granular particles (with or without a liquid substrate) at different rates. Because of this, a multicomponent sample injected into a chromatograph will elute as a series of separate chemical species.

In the present studies, a packed column is operated isothermally with a constant flow rate of carrier gas (helium). A sample is injected into the carrier gas and as it passes into the chromatograph, the various species diffuse, adsorb, and desorb. For each chemical, axial diffusion is represented by the Peclet number, mass transfer to the adsorbent surface is represented by the parameter N_{tOG} , and adsorption-desorption is represented by the thermodynamic parameter mR_0 . The Peclet number is a function of both the fluid mechanics and physical properties of the system;

N_{t00} is primarily a function of the fluid mechanics; and mR_0 is a function of the chemical species and the column used.

PART II

SUMMARY

An existing gas chromatograph test facility has been operated isothermally to generate data on both single component and binary mixtures of n-pentane and n-heptane. A previously developed chromatographic data reduction computer program and an equilibrium adsorption model were used to analyze the data.

Binary data obtained on a porous column shows that superposition of predicted single component behavior is only a first order representation of actual binary data. The parameter mR_0 is found to be a linear function of composition. This suggests that the adsorption follows a non-linear isotherm, and that there are possible interference effects in binary systems.

Data obtained on a non-porous column is well predicted by the model, and fails to show spreading that was observed on porous columns. This shows that the mechanism of intraparticle diffusion is responsible for the observed spreading.

The porous packing, C-102, was found to consist of porous microspheres. The manufacturer reports an average micropore diameter of 90 Å, while experimental results show the macropores range from 400-700 Å.

A system of automatic data processing was evaluated and found to offer less accuracy than possible with the present manual processing. Minor changes in the detector control circuit are recommended to improve manual data handling.

PART III

BACKGROUND

Previous work on the gas chromatograph system includes development of several mathematical models (1,2,4,6). Each model was developed from the fundamental second-order partial differential equation set describing the chromatograph, and each predicts the behavior of a single component sample at the column outlet based on an impulse injection. Two second-order models which include axial diffusion have been developed, the equilibrium adsorption model (2) and the non-equilibrium adsorption model (4,6). The former assumes pointwise adsorption equilibrium throughout the column ($N_{tOG} = \infty$), while the latter assumes a non-equilibrium situation ($N_{tOG} = \text{finite}$). Woodrow (6) has shown that, for the conditions of the test facility used, the non-equilibrium model offers only minor improvement in prediction of output chromatograms. Because of this, and because the non-equilibrium model requires more extensive calculations, the equilibrium adsorption model is used for data analysis in this report. This model assumes pointwise equilibrium between the gas phase and the adsorbed phase of the packing, i.e., the column is very long. The equilibrium adsorption model is represented by

$$y_g(\theta, 1) = \sqrt{\beta Pe / 4\pi \theta^3} \exp \left[-Pe(\theta - \beta)^2 / 4\beta \theta \right]$$

which gives the response at the end of the column to a unit impulse.

To obtain experimental data, a previously built test facility was used (5). The data are analyzed using a general data reduction computer program (GDRP) prepared by Benoit (5), which

given chromatographic input data, output data, and system parameters such as the Peclet number and N_{t00} , will reduce the data to dimensionless form, predict an output chromatogram based on the model, and numerically and graphically compare the prediction with the actual data. This program predicts chromatograms for finite pulse injection by numerically convoluting the input data with the calculated impulse response. The physical parameters (Pe , N_{t00} , Re , v , etc.) are calculated by another computer program (6).

In order to extend the model to multi-component systems, superposition of single component chromatograms has been investigated by Keba (6). His work has shown that superposition offers only a first order approximation of actual binary data, and that the parameter mR_0 is apparently composition dependent. Further work has been done on binary systems in order to verify this result and to determine the variations of mR_0 with composition.

The data of Benoit (5) and Keba (6) has shown spreading of the output chromatograms that is not predicted by the model. Since a porous packing was used in obtaining this data, it has been postulated that this spreading is due to intraparticle diffusion(6). In order to study this, data have been obtained on a non-porous column.

Work is being done by Woodrow (7) to improve the mathematical model to obtain more accurate prediction. This requires data on the physical characteristics of the adsorbents, such as particle pore size distribution and column void fraction. Preliminary

estimates of these properties were obtained from experimental work and from manufacturer's literature.

In an attempt to improve consistency in the data and to reduce the manual effort in handling the data, a method of automatic data processing was investigated.

PART IV

RESULTS AND DISCUSSION

A. SUPERPOSITION AND BINARY DATA

The mathematical model assumes a linear isotherm for each component of the form (1)

$$y^* = mx_L.$$

This is generally a valid assumption if the sample composition in the carrier gas is small. For a typical sample used in this work, the sample compositions are on the order of 10^{-2} mole fraction (see Appendix A).

This isotherm implies that equilibrium for each component is independent of any other components present. Because of this, it seems reasonable to use a linear superposition of the single component predictions to predict the behavior of a binary mixture.

Data on the binary system of n-pentane and n-heptane were obtained on the porous Chromosorb 102 column (C-102) described in Table I, at 150°C, 175°C, and 200°C. The sample compositions ranged from an excess of pentane to an excess of heptane. In all cases a syringe was used for injection of two microliter liquid samples. The experimental conditions for the binary data are given in Table II.

Analysis of binary data shows that the time of appearance of the output peaks in binary mixtures lags the time predicted from superposition of pure component predictions. This effect is shown for a typical experiment in Figure 1. This time lag

TABLE I

COLUMN CHARACTERISTICS

	Chromosorb 102	Carbowax 1500
Length (cm)	100	100
Outside Diameter(cm)	0.32	0.32
Inside Diameter(cm)	0.22	0.22
Mesh	60/80	60/80
Particle Size(cm)	0.025/0.0177	0.025/0.0177
Composition	Microporous Styrene-Divinyl Benzene Polymers	Polyethylene Glycol 20% by weight
Temperature Range	Room-250°C	Room-150°C
Application	Separation of low molecular weight, very polar sub- stances such as water, alcohols, amines, acids, esters, ketones, ethers, aldehydes, and to a limited extent, light gases.	Separation of high boiling polar com- pounds. General purpose column for polar samples.

TABLE II

EXPERIMENTAL CONDITIONS
FOR BINARY DATA ON C-102

Temperature deg C	Column Inlet Pressure, psig	Helium Flowrate [*] cu cm/min
150	30.0	29.4
175	30.0	30.0
200	30.0	26.4

^{*} at 70°F and 14.7 psia

occured for both components for all mixtures and at all temperatures. It was found that the time lag increased as the component composition became more dilute. (see Table III)

The peak time is primarily related to the thermodynamic parameter mR_0 (2). This parameter cannot be estimated a priori and is determined from actual data by a curve fitting technique which varies mR_0 until the peak time of the predicted chromatogram matches the peak time of the output data (5). To determine mR_0 values for binary chromatograms, the output of each component is analyzed separately by use of the GDRP. By use of this method, mR_0 values have been calculated for each component. As a general trend, the value of mR_0 decreases as the component becomes more dilute at constant temperature. From Figures 2 and 3, mR_0 is seen to be a linear function of composition. It should be noted that some binary samples (75% and 99% pentane by weight) were not sufficiently separated at 200°C on C-102, so mR_0 values could not

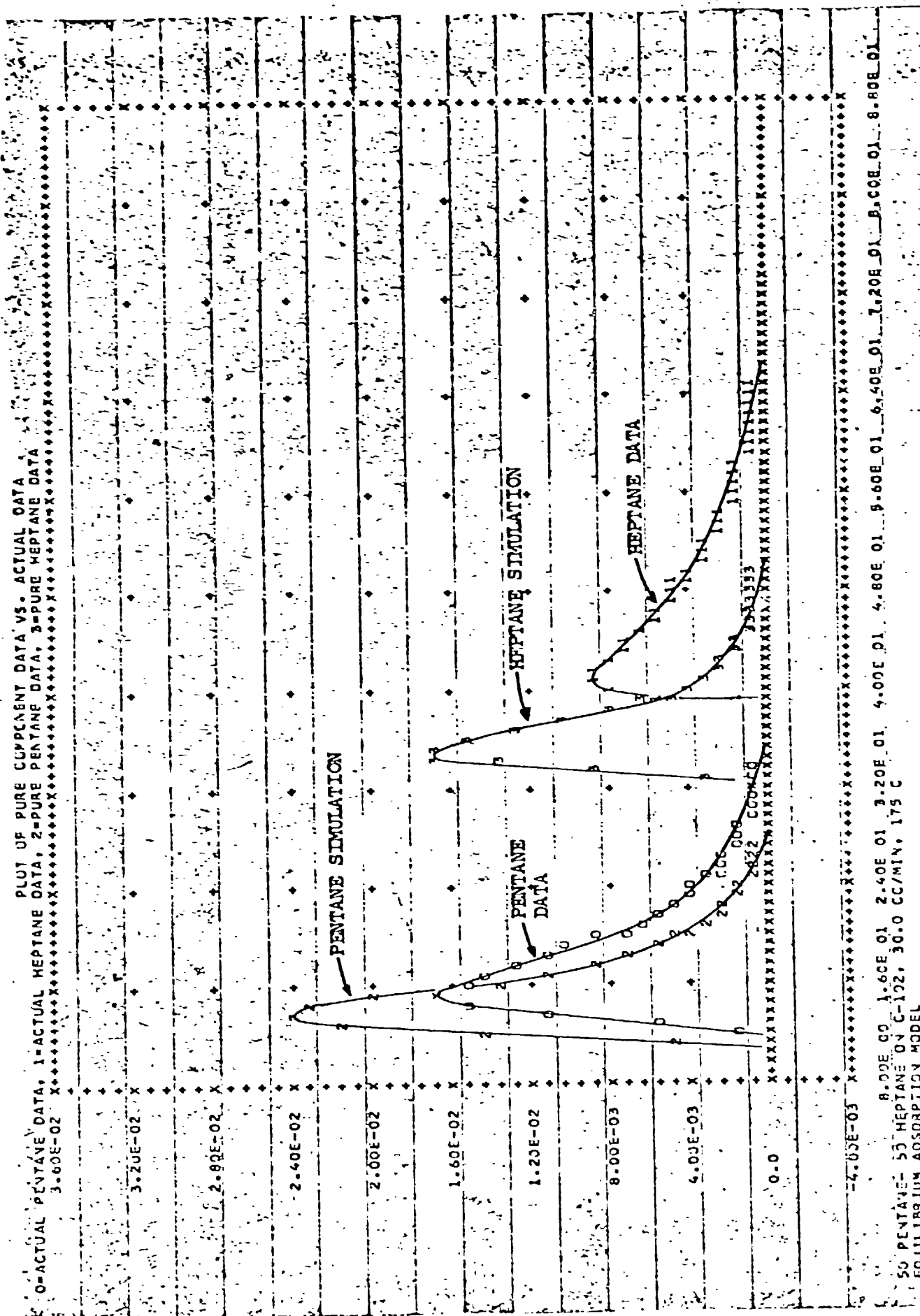


Figure 1 Predicted and Actual Binary Chromatograms
 for Pentane-Heptane System on C-102 at 175°C

TABLE III

TIME LAGS IN BINARY DATA

Pentane-Heptane System on C-102
Flow Rate of 29.4 cc/min at 150°C

Composition weight %	Time of Pentane Peak, sec	Time of Heptane Peak, sec
100 H	-	285.5
99 H - 1 P	95.0	294.0
75 H - 25 P	88.5	307.5
50 H - 50 P	85.0	327.5
25 H - 75 P	84.0	364.0
1 H - 99 P	81.5	432.5
100 P	80.5	

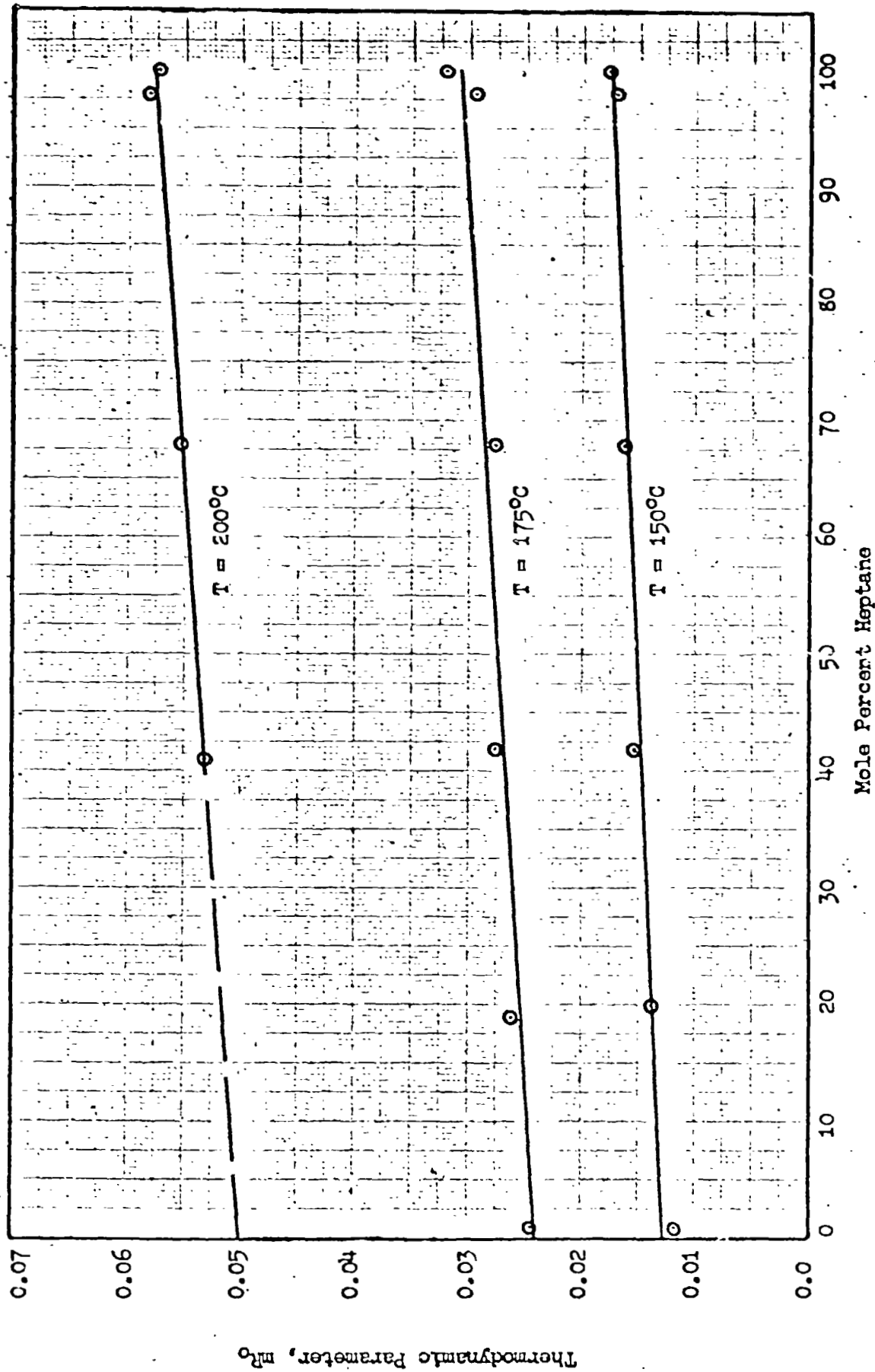


Figure 2 Effect of Composition on Heptane mR_0 for Pentane-Heptane System on C-102

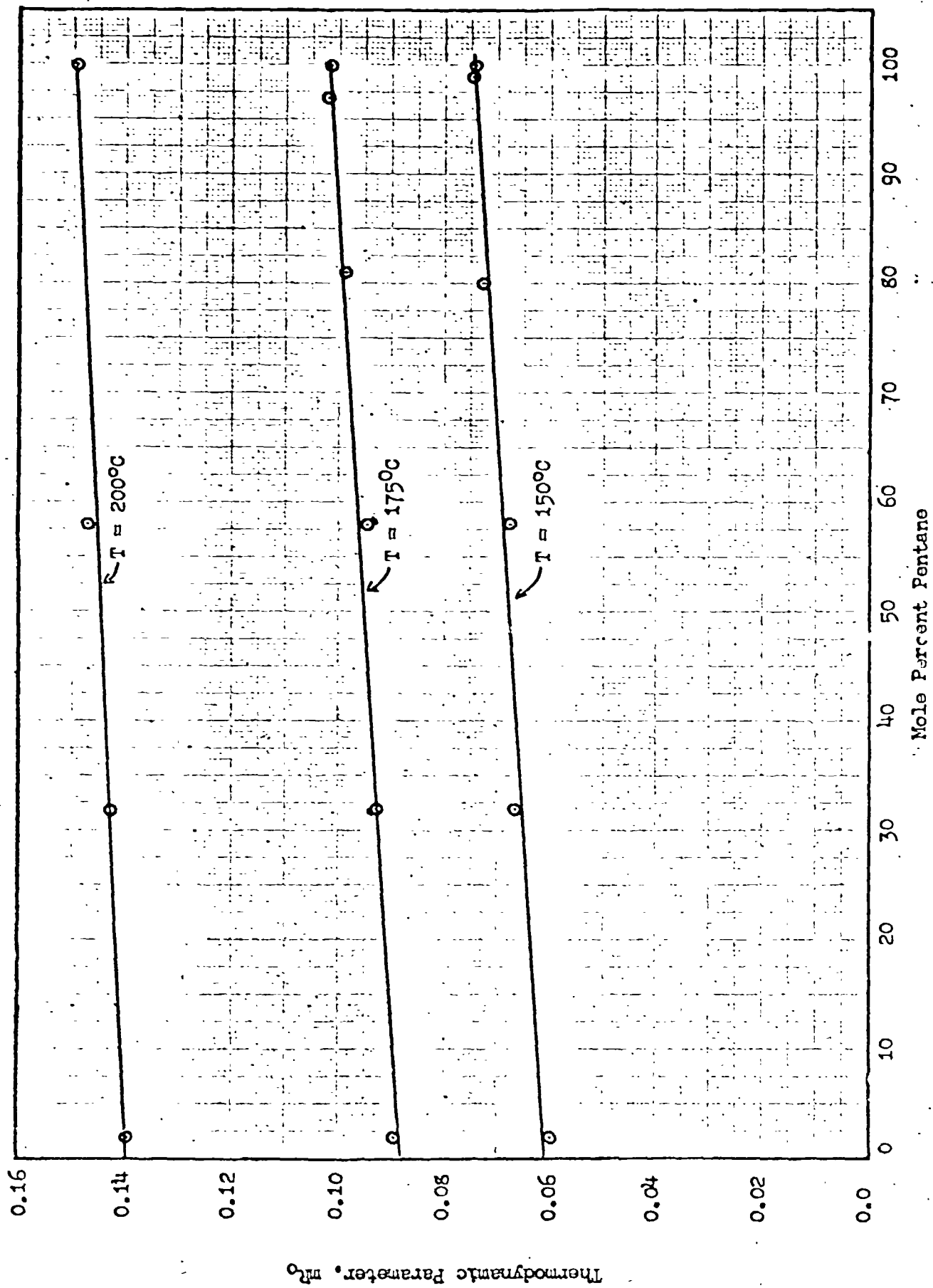


Figure 3 Effect of Composition on Pentane mR_0 for Pentane-Heptane System on C-102

be calculated for these samples.

Since Keba (6) also noted the occurrence of a time lag, mR_0 values were estimated for his data on C-102 at 150°C and 200°C by means of the following relation (5)

$$mR_0 \approx \frac{1}{\theta_{\max,0} - \theta_{\max,1} - 1}$$

which gives a value within $\pm 10\%$ of the actual value. These values appear in Figures 4 and 5, and it can be seen that the same general trends are exhibited.

There are several possible reasons for the observed behavior of the parameter mR_0 . First, the observed variations with composition are probably due to changes in the equilibrium constant m , since R_0 is essentially constant at constant temperature and pressure. This indicates either that the isotherm is not linear as assumed but there is no interference effect, or that the isotherm is non-linear and dependent upon the concentrations of both components.

The first explanation makes use of the fact that, since the binary samples were all two microliters, the composition of a component in the carrier gas decreases as its composition in the sample decreases. A typical non-linear non-interactive isotherm is

$$x_{L,1} = \frac{K y_1^*}{1 + K y_1^*}$$

a Langmuir, single-component isotherm. This isotherm would give

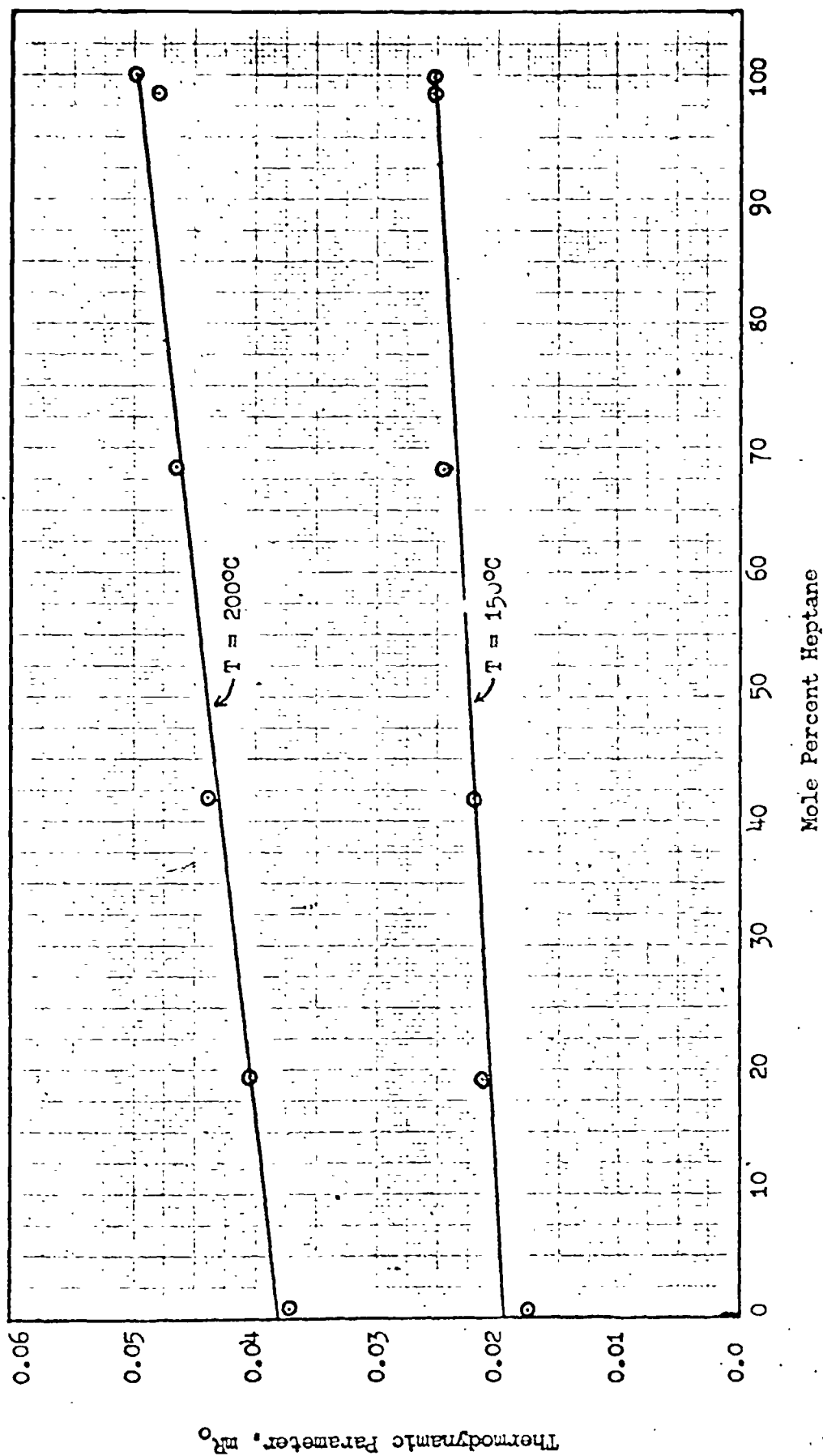


Figure 4 Effect of Composition on Heptane m^0
for Pentane-Heptane System on C-102
(Data of Keba)

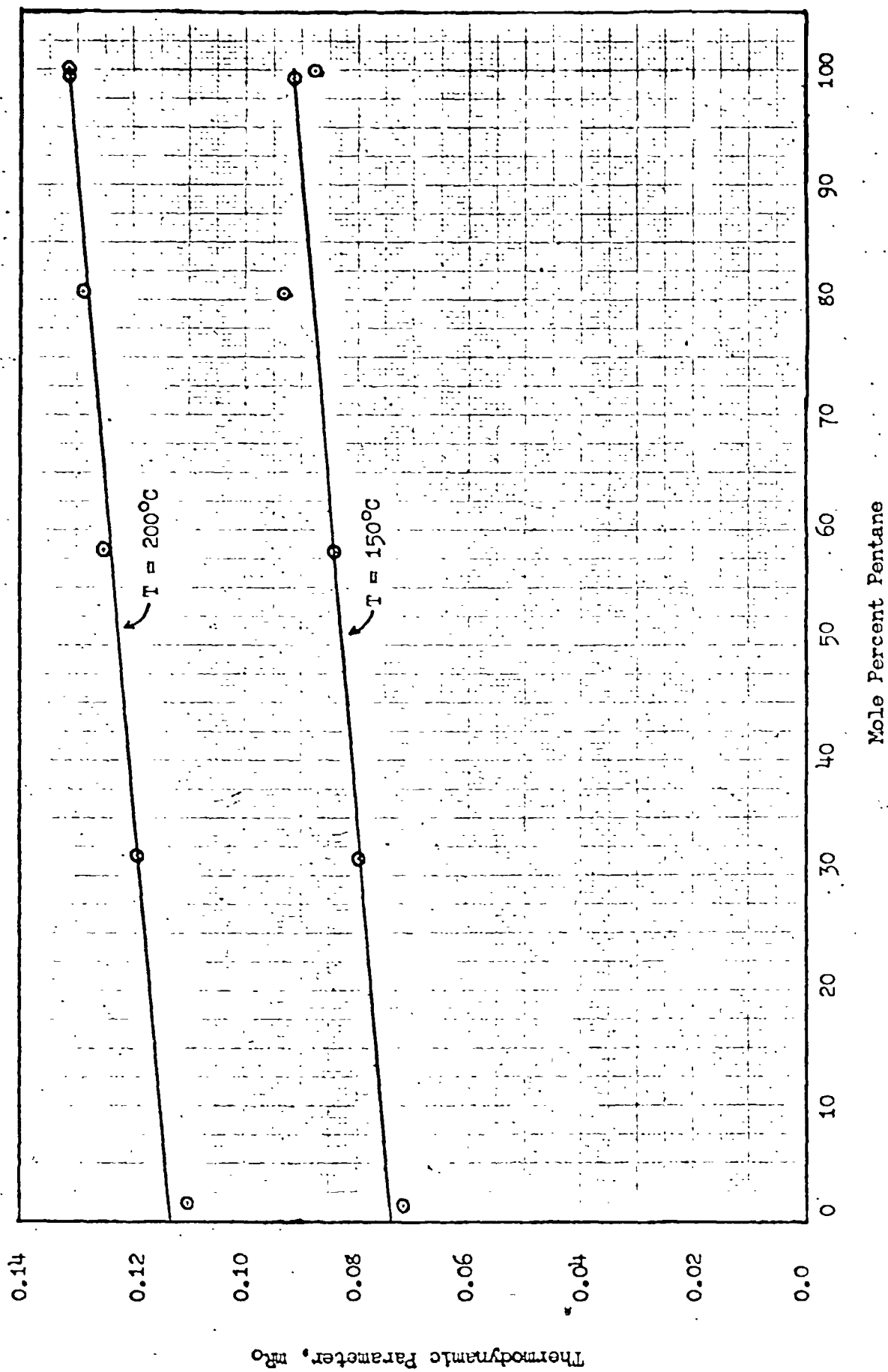


Figure 5 Effect of Composition on Pentane mR_0
for Pentane-Heptane System on C-102
(Data of Keba)

a different value of m for each value of y^* , but does not include any effect of another component. If the adsorption followed this isotherm, changes in the pure component injection volume would produce variations in the value of m . Specifically, if y^* is reduced, m will decrease, which is consistent with the observed effect. If this is indeed the case, the above equilibrium relation can be used in the mathematical model, and superposition can be used to predict binary data, although its use is not rigorously correct. Use of this non-linear isotherm would considerably complicate the calculations. It may not be possible to obtain an analytical solution, and numerical methods may be required.

Any interference effect in the binary systems is probably in the form of competition between the two components for adsorption sites. This can be represented by a non-linear interactive isotherm

$$x_{L,1} = \frac{K_1 y_1^*}{1 + K_1 y_1^* + K_2 y_2^*}$$

a binary Langmuir isotherm. The calculations for this non-linear interactive model are not much more complicated than those for the non-linear, non-interactive model. Use of this model, if it is correct, would predict binary chromatograms and the assumption of superposition would not be required.

B. TEMPERATURE EFFECTS

In general, the value of mR_0 increases as the temperature increases. The form of this temperature variation has been proposed as (6)

$$mR_0 \propto \exp(-E/RT) .$$

Correlation of pure component C-102 data according to this expression is given in Figure 6. Over the limited temperature range considered, the data does follow the correlation and activation energies on C-102 are on the order of 11 kcal/gm-mole for pentane and 15 kcal/gm-mole for heptane. These values indicate that the controlling mechanism is probably the physical adsorption process. Pentane is well modeled even at 150°C (Figure 7), but the quality of prediction for the heptane data increases at higher temperatures as shown in Figures 8, 9, and 10 (see Appendix B for computer output). This substantiates the fact that physical adsorption is controlling.

C. PRESSURE DEPENDENCE OF mR_0

The parameter mR_0 consists of two separate factors: m , an equilibrium adsorption constant; and R_0 , the ratio of moles of gas in the bed to moles of liquid in the bed.

The parameter m appears as a result of the assumption of a linear isotherm. This is expressed as

$$x_L = Kp^* ,$$

but assuming an ideal gas (g) one obtains

$$x_L = KPy^*$$

or

$$y^*/x_L = 1/KP = m .$$

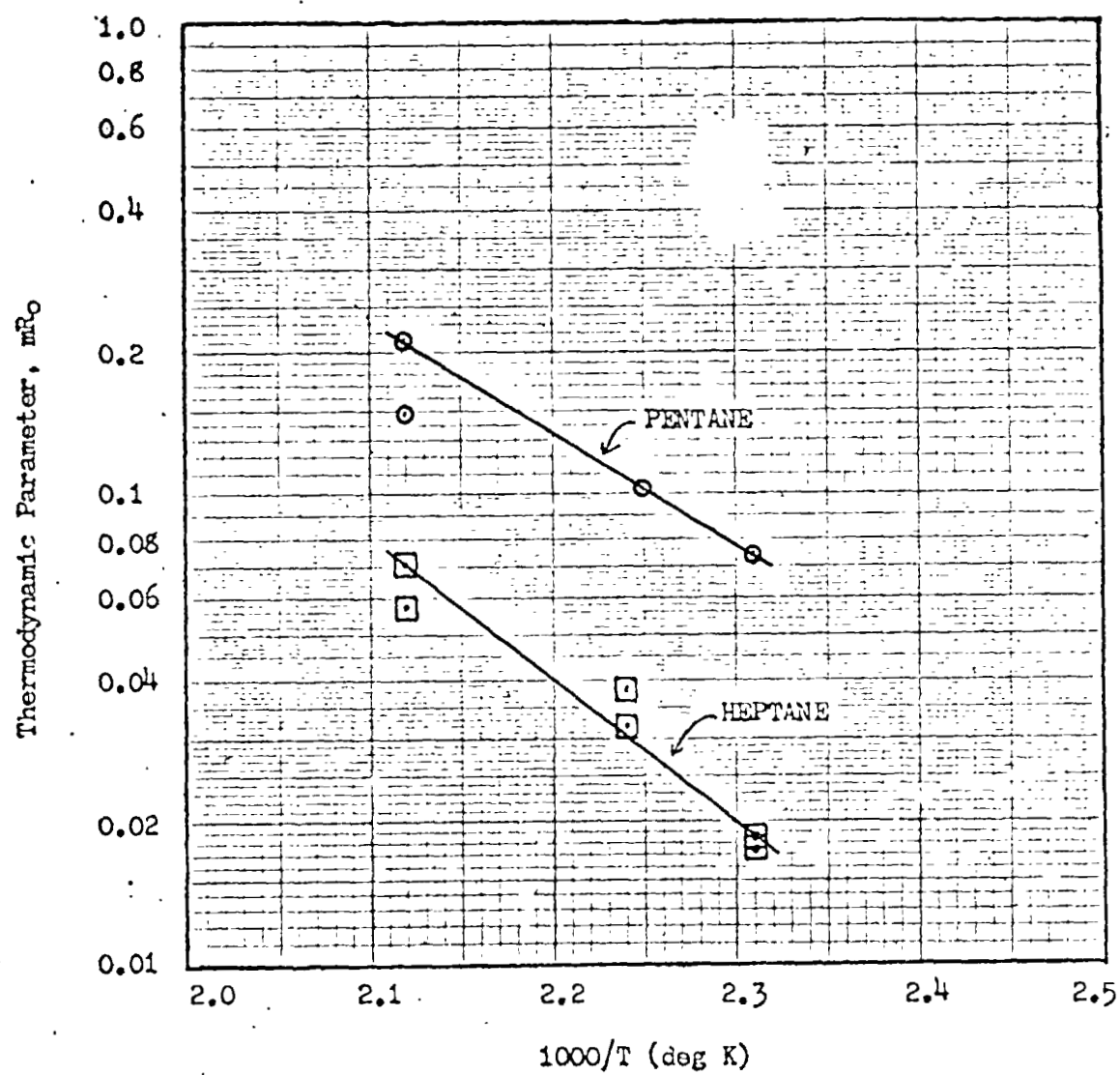


Figure 6 Effect of Temperature on
Parameter mR_0 for C-102

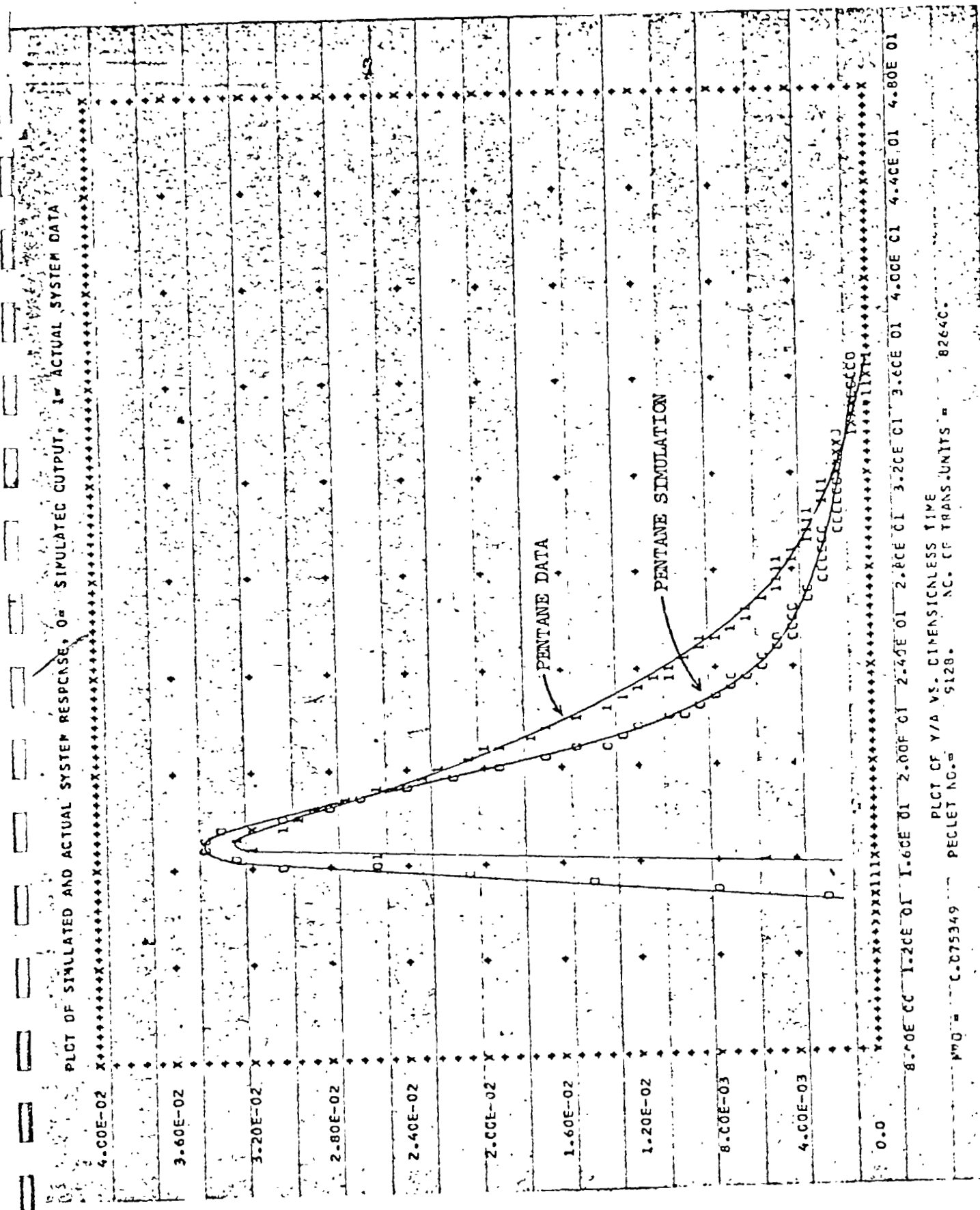
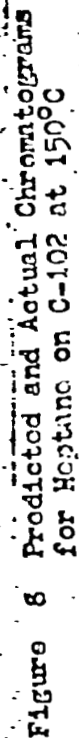


Figure 7 Predicted and Actual Chromatogram for Pentane on C-102 at 150°C



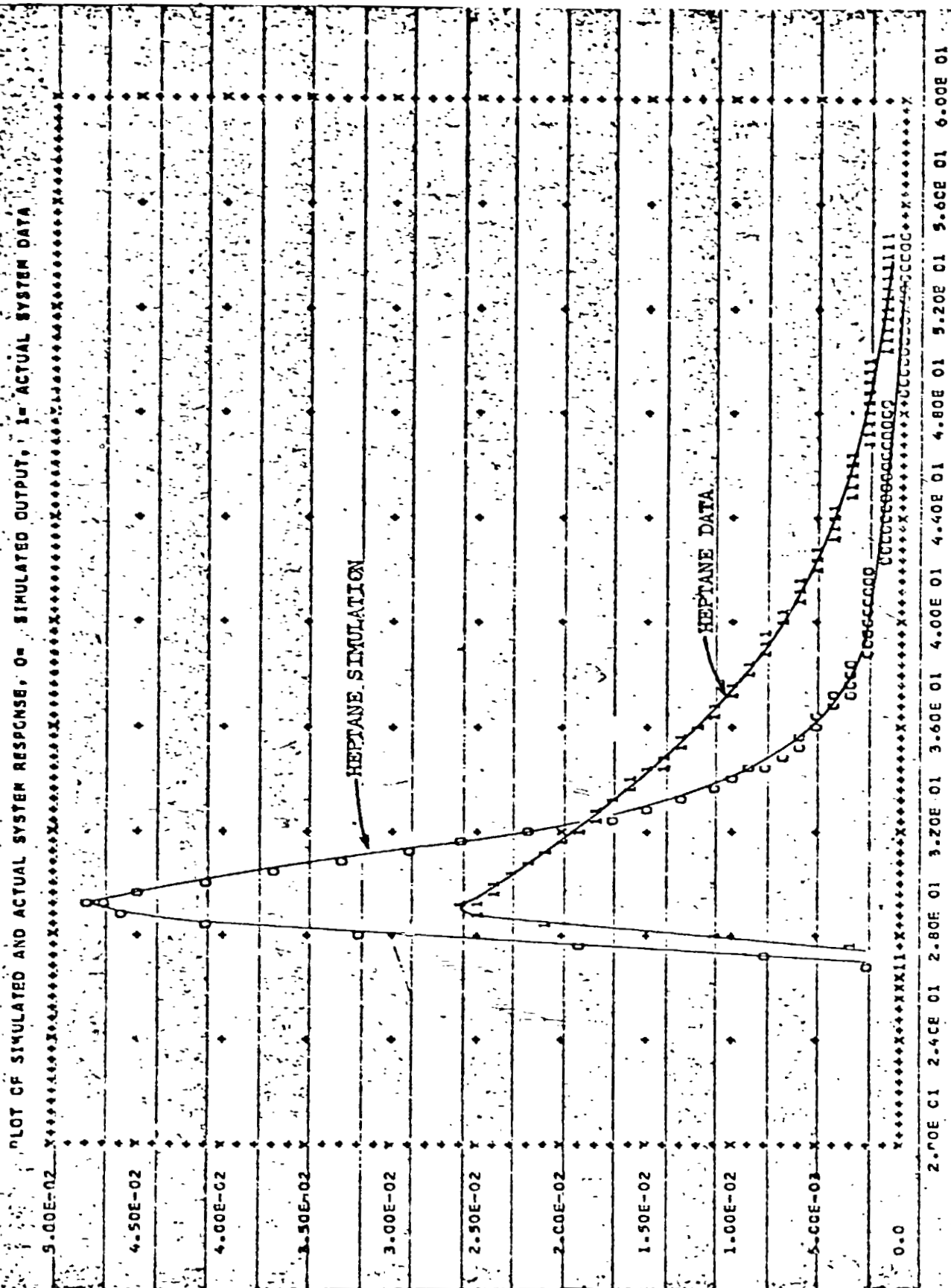


Figure 9 Predicted and Actual Chromatograms for Heptane on C-102 at 175°C

If K is assumed to be independent of pressure, m is seen to be inversely proportional to pressure.

The parameter R_0 is defined as (1)

$$R_0 = \epsilon \rho_c / F(1-\epsilon) \rho_L$$

For an ideal gas, the density is proportional to pressure (at constant temperature). The void fraction of the bed is independent of pressure. F is the stationary phase volume which is liquid. Both this term and the liquid density are very weak functions of pressure.

Combining these effects, one obtains

$$mR_0 = m\epsilon \rho_c / F(1-\epsilon) \rho_L \propto (1/P)(P) \propto P^0$$

Therefore, as a rough estimate, one would expect mR_0 to be independent of pressure. This is borne out by the data obtained (see Figure 6).

D. DATA ON NON-POROUS PACKING

A Carbowax 1500 column (C-1500) described in Table I, which is believed to approximate a non-porous packing, was used to generate single component data for pentane, heptane, and acetone. The experimental conditions for this data are given in Table IV. It is seen in Figures 11 and 12 that the model very closely predicts the shape of the actual data. This indicates that the presumed mechanism of intraparticle diffusion is probably responsible for the observed spreading of the porous column data.

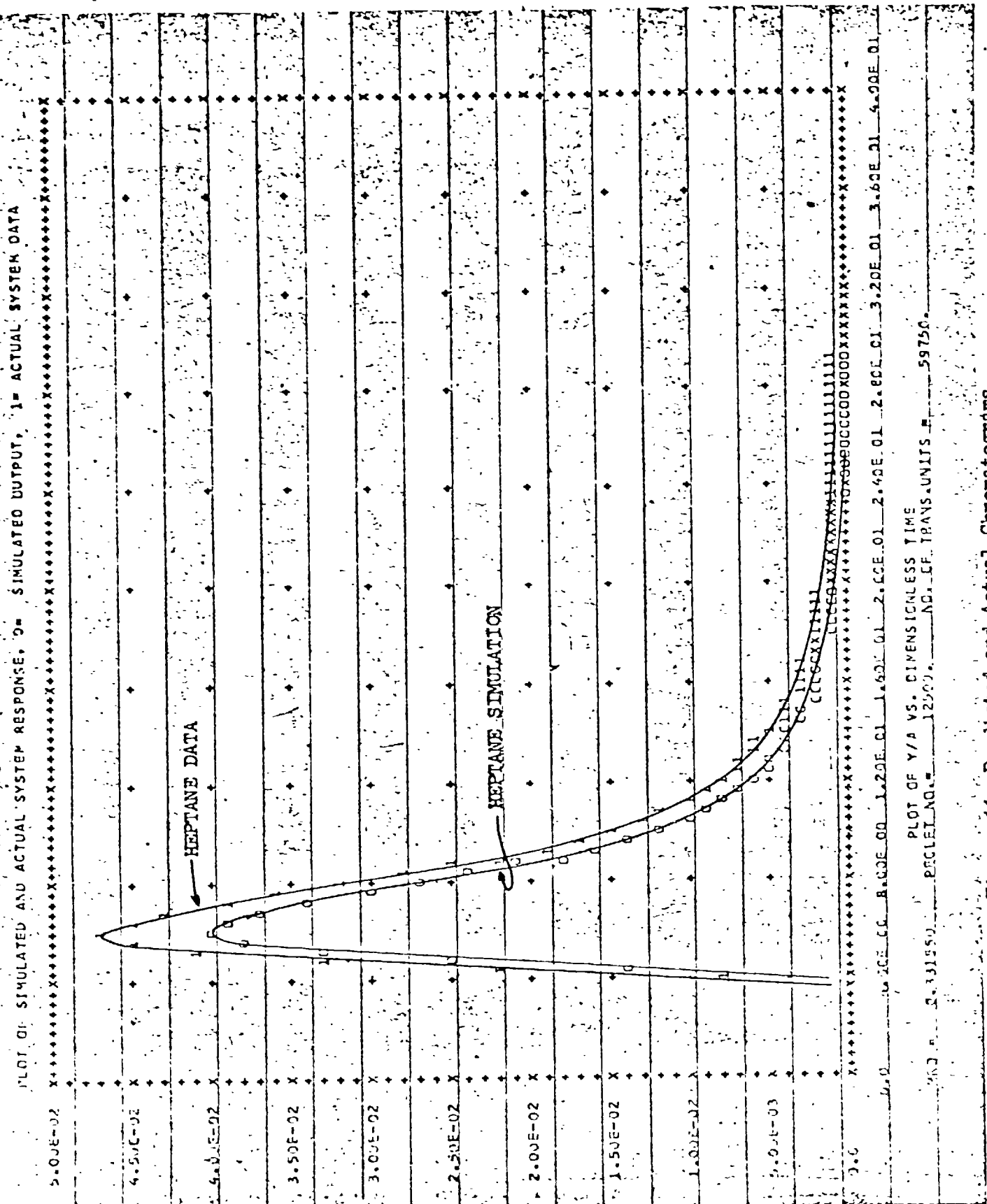
TABLE IV

EXPERIMENTAL CONDITIONS
FOR DATA ON C-1500

Temperature deg C	Column Inlet Pressure, psig	Helium Flowrate* cu cm/min
100	20.0	31.8
125	20.0	29.6
150	20.0	27.7

* at 70°F and 14.7 psia

Analysis of these data presented some problems. Pentane and heptane are weakly adsorbed on C-1500, resulting in a very sharp impulse response. However, there is much tailing in both the input and output data so a relatively coarse time step was used in the computer analysis. The combination of these two factors accounts for the failure of the convolved response to predict exactly the height of the actual data in the two figures (11 and 12) shown. The actual area under the convolved response is somewhat less than that under the actual chromatogram. Since the area under the curve is proportional to the amount of the sample injected, both of these areas should be the same for proper prediction. Because of this, each value of the convolved response should be multiplied by a constant so that the area under this curve is identical to the area under the actual data. It can be seen that if this were done, the two curves would be virtually identical.



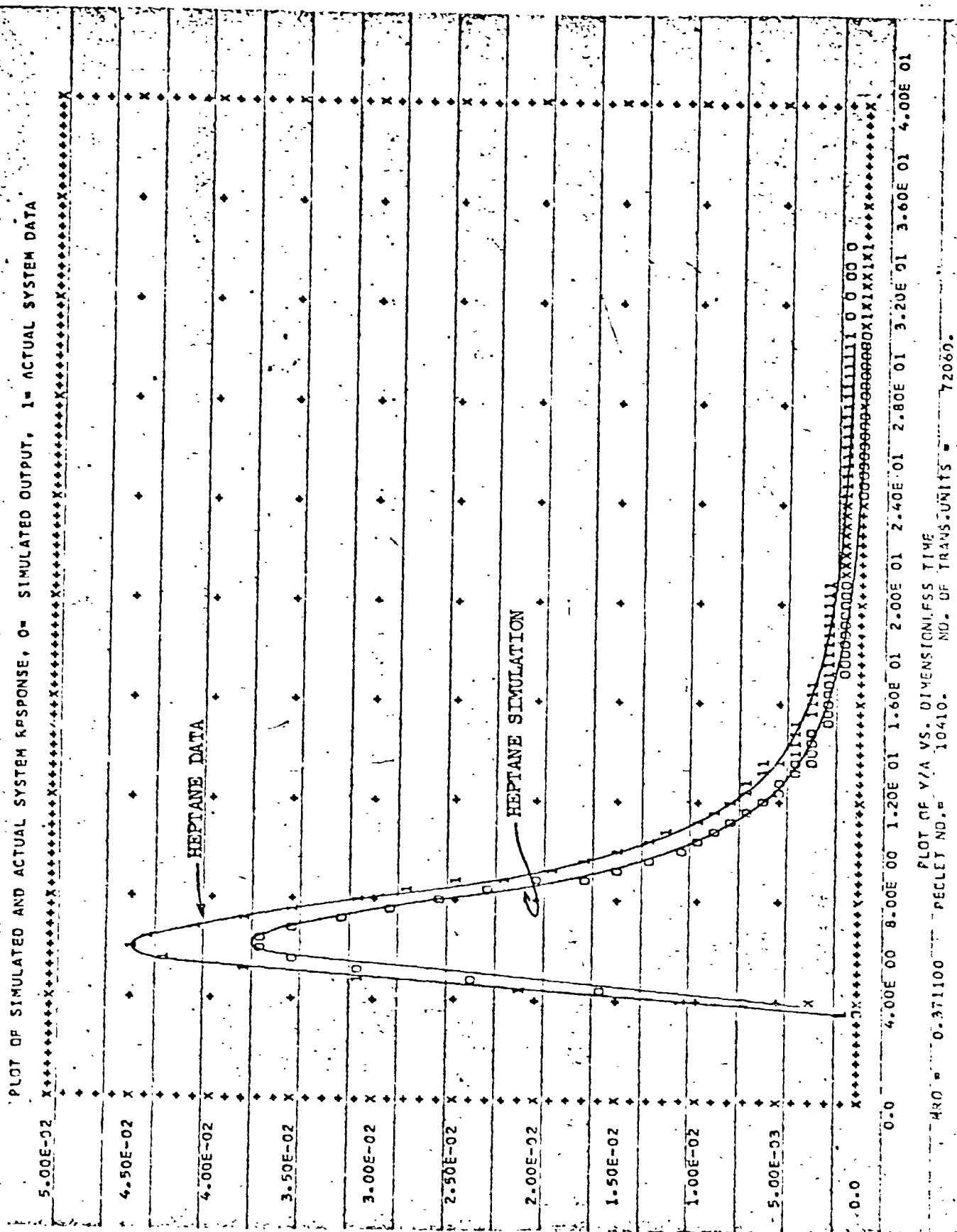


Figure 12 Predicted and Actual Chromatograms
for Heptano on C-1500 at 150°C

The observed oscillations at the end of the convolved response (Figure 12) are probably due to the large time step used and errors in the data (see following section). These oscillations are inconsequential in the determination of mR_0 and the predicted response.

Over the range of temperature studied, the C-1500 column would not separate the binary mixtures of pentane-heptane. In order to obtain a qualitative estimation of the degree of separation obtained, moment analysis was used. Voytus (2) has shown that the time of the center of gravity of a chromatogram (mean), as well as the variance, can be obtained by moment analysis from the Laplace transform solution of the model and knowledge of the system transport parameters. The mean is defined as

$$\bar{\theta} = \frac{\int_0^{\infty} \theta y \, d\theta}{\int_0^{\infty} y \, d\theta}.$$

The variance, or second moment about the mean, is

$$\sigma^2 = \frac{\int_0^{\infty} (\theta - \bar{\theta})^2 y \, d\theta}{\int_0^{\infty} y \, d\theta}.$$

For the equilibrium adsorption model, it has been shown (2) that

$$\bar{\theta} = \beta = 1 + 1/mR_0$$

and

$$\sigma_f^2 = \beta^2(2/Pe),$$

where σ_g^2 is the variance of the impulse response. The variance of an actual chromatogram (9) is

$$\sigma^2 = \sigma_g^2 + \sigma_I^2$$

where σ_I^2 is the variance of the input pulse. The value of σ_I^2 is obtained from actual input data using the defining equation given above. Values of σ_I^2 for the input data of Keba have been calculated (7) and are used in this analysis. Voytus (2) has shown that at least 94 % of the total area of the chromatogram is within a 2σ spread about the mean.

The analysis done here is for the pentane-heptane system at 100°C. Pure component values of mR_0 were used and the binary system was represented by superposition of the two pure component predictions. Table V summarizes the values of the parameters used.

TABLE V
PARAMETER VALUES FOR
MOMENT ANALYSIS

	mR_0	Pe	σ_I^2, sec^2	σ_g^2, sec^2	σ^2, sec^2	$2\sigma, \text{sec}$
Pentane	0.4566	10780	19.63	0.03	19.66	8.88
Heptane	0.3315	12500	19.63	0.04	19.67	8.88

The chromatograms were assumed to be approximately symmetrical about the mean (implying that the mode is about equal to the mean). With these assumptions, the semi-qualitative Figure 13 was drawn (see Appendix C for calculations). It shows the great degree of overlap of the pentane and heptane chromatograms, and that, while some separation occurs, it would not be detectable.

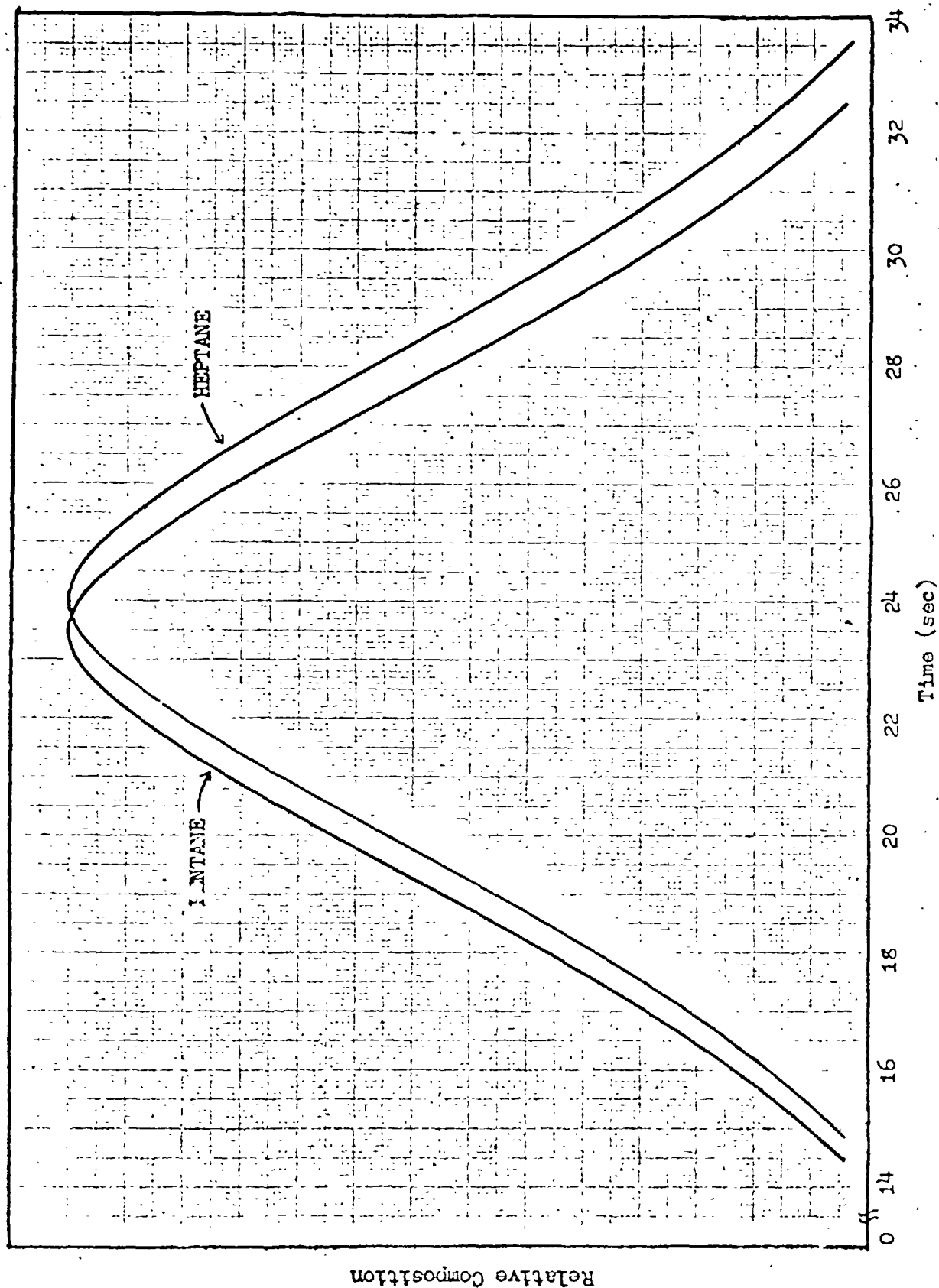


Figure 13 Prediction of Pentane and Heptane Chromatograms for a Binary Mixture Using Moment Analysis

The temperature behavior of the C-1500 data is shown in Figure 14, which presents only a quantitative representation. It is obvious that the straight lines drawn are subject to a large degree of error, since there are so few data points. The value of mR_0 for acetone and heptane increases as temperature increases, while the value for pentane remains relatively constant over the temperature range studied. The mR_0 values for pentane and heptane diverge as the temperature decreases, indicating that a detectable separation might occur at a temperature below 100°C. The activation energies for pentane, heptane, and acetone on both C-1500 and C-102 are given in Table VI (see Appendix D for calculations). The energies are much lower for the C-1500 column than for the C-102. This is because the components are very weakly adsorbed on the C-1500. This could also explain the erratic behavior of the pentane and heptane mR_0 .

TABLE VI
ACTIVATION ENERGIES
kcal/gm-mole

	C-1500	C-102
Pentane	0.	11.
Heptane	0.5	15.
Acetone	2.0	6. (Ref. 6)

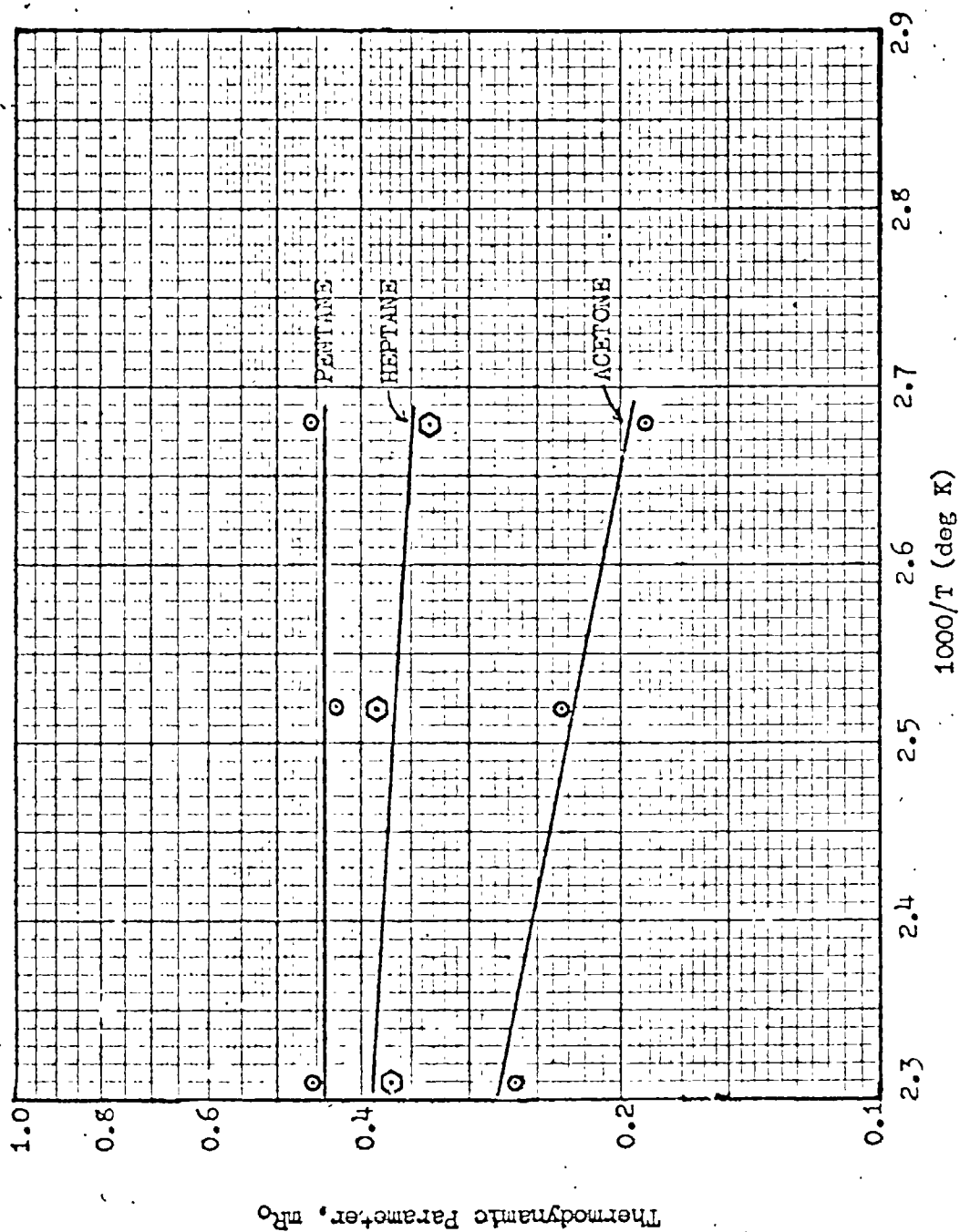


Figure 14 Effect of Temperature on Parameter mR_0 for C-1500

E. SOURCES OF ERROR

Since the data are presented in a form which requires computer calculations, there are many sources of error. Errors are associated with reading the value of the chromatogram from the strip chart (see Part IV, G), assuming isothermal column operation, determining helium flow rate, estimating the various parameters (P_e , N_{tO_2} , R_e , etc.), using numerical methods in computer calculations, and with computer roundoff. When the parameter mR_0 is calculated, all these errors are present. Since mR_0 is determined by a curve fitting technique, the major source of error is in the processing of the actual data.

Each data point has two dimensions associated with it: composition and time. The height of the trace on the strip chart above the base line is proportional to the composition (y) of the component in the carrier gas. This height is measured using an engineer's rule so the error here is ± 0.02 inch. Since the maximum deflection obtained was about 3 inches for most of the experiments, the average error is about 1%. For the data studied in this report, a value of y is read every half second. Since time lines appear only once a second on the strip chart, there is an error in estimating the time of about ± 0.1 second. Another error associated with time is the location of "zero" time. This is generally taken to be the time of appearance of the input pulse, but since values are taken only once every half second, there can be an error of as much as 0.4 second. The manner in which these errors are propagated in the calculations is difficult

to determine, although it seems likely that the value of mR_0 obtained is only accurate to within $\pm 20\%$.

Possible ways to reduce this error are in obtaining a full scale deflection on the strip chart (see Part IV, G) and using a time line of 0.1 second. The latter is possible if the paper speed is increased to the next faster speed, 1 in/sec. This reduces the error in determining the time associated with a point, but uses the light sensitive paper at five times the current rate. As this paper is expensive, the improvement brought about by such a change should be evaluated carefully to determine if it is justified.

F. PACKING CHARACTERISTICS

An effort was made to obtain the physical characteristics of the C-102 and C-1500 packings used. Information on composition and particle size appear in Table I.

It was found that C-102 is manufactured by the Rohm and Haas Company under the trade name "Amberlite XAD-2" and that Perkin-Elmer merely dries and crushes it before packing the columns (10). A technical bulletin and sample of XAD-2 were obtained from Rohm and Haas, and a sample of C-102 was obtained from Perkin-Elmer. The structure of XAD-2 appears in Figure 15, while some of its properties are listed in Table VII. From the concept of Figure 15, it is postulated that each particle consists of a large number of very small microspheres, which, in turn, are porous.

The C-1500 packing consists of firebrick (manufactured by

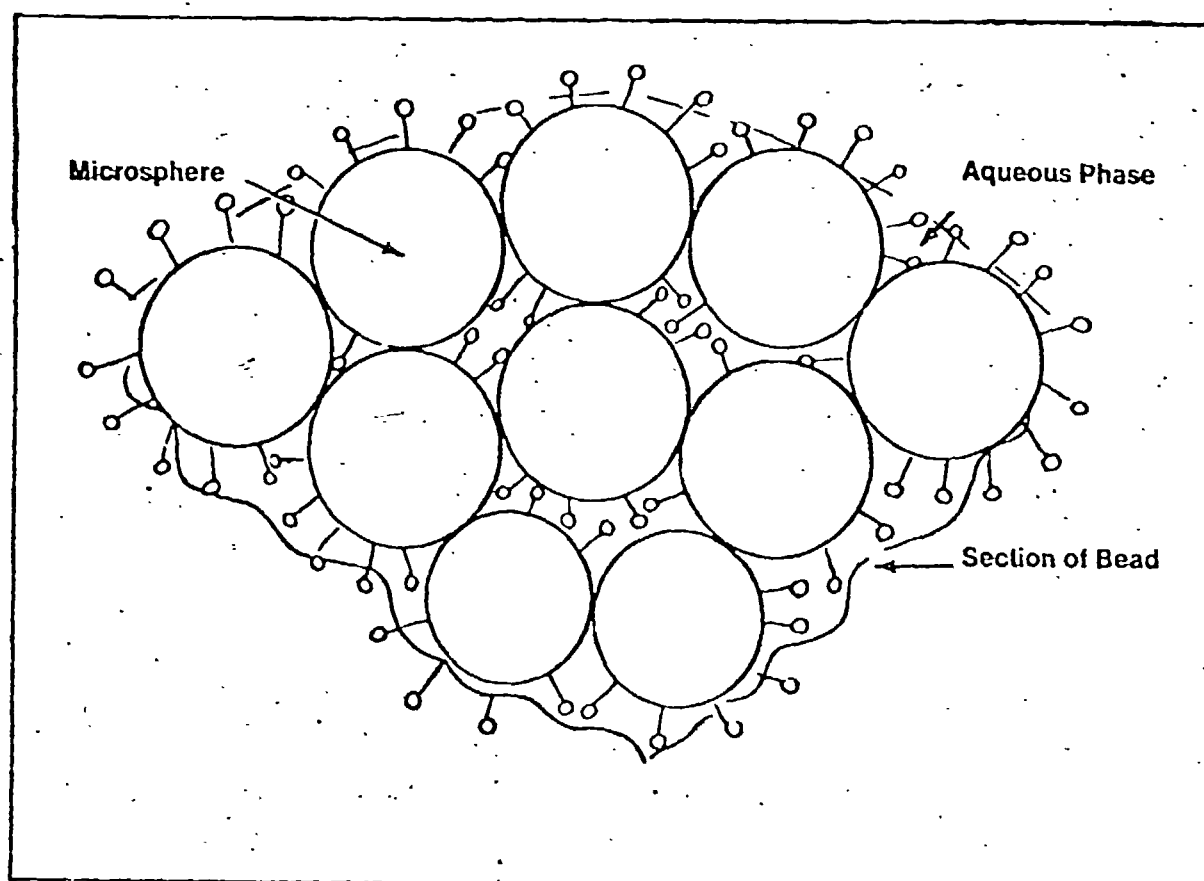
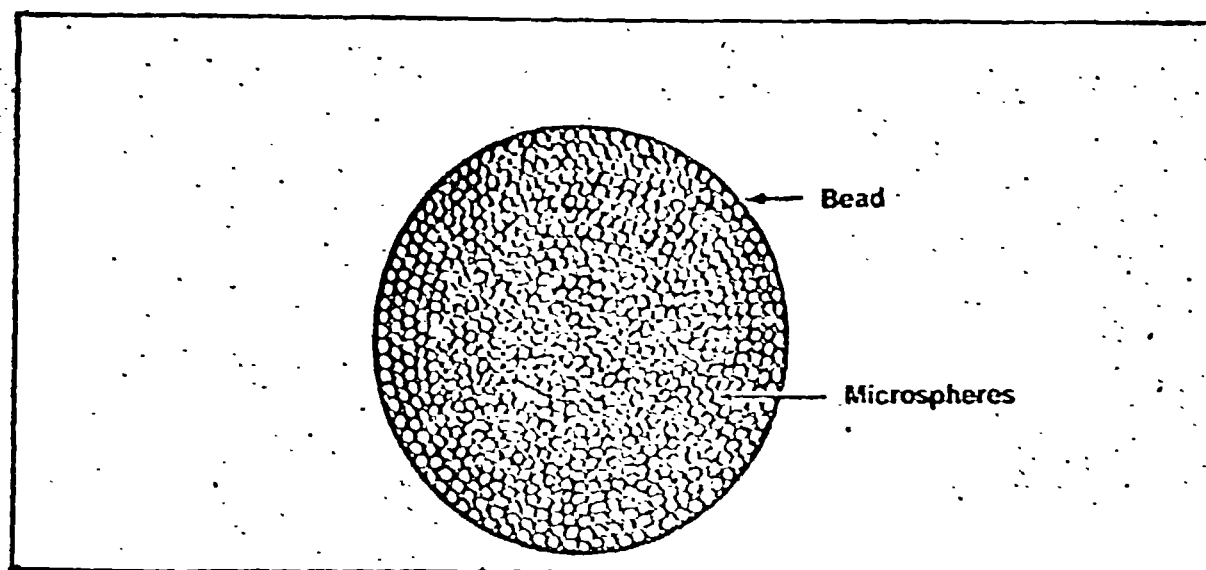


Figure 15 Structure of XAD-2
(From Rohm and Haas
Technical Bulletin,
Reference 11)

TABLE VII

PROPERTIES OF XAD-2
(Reference 11)

Appearance	Hard, Spherical opaque beads.
Solids	51 to 55
Porosity(ml pore/ml bead - dry basis)	0.40 to 0.45
Surface Area(m ² /gm - dry basis)	330
Effective Size (mm)	0.30 to 0.45
Harmonic Mean Particle Size (mm)	0.45 to 0.60
Average Pore Diameter (A - dry basis)	90
True Wet Density in distilled water (gm/ml)	1.02
Skeletal Density (gm/ml)	1.07
Bulk Density (lbs/ft ³) (gm/cc)	40 to 44 0.64 to 0.70
Bulk Density* (gm/ml)	0.40

* experimentally determined. It is assumed that the bulk density reported by Rohm and Haas is the density as shipped, i.e., about 50% wet.

Union Carbide) doped with polyethylene glycol by Perkin-Elmer (10).

A sample of this packing was also obtained.

A mercury penetration porosimeter was used to estimate actual pore distribution and external void fraction of these samples. It is probable, however, that the results obtained are subject to large errors, as the proper sample holder for these powder samples was not available. The available sample holder, designed for large pieces of material, was used and the results are considered to be semi-quantitative. The results of the tests for XAD-2 and for C-102 appear in Figures 16 and 17 respectively. Meaningful results were not obtained with the C-1500 sample, because some of the sample flowed out of the holder during the experiment.

In Figure 16, the section of the curve up to about 100 psia represents the external void volume, while the region between 1000 psia and 10,000 psia represents the macropores within the particles (most probably the volume between the microspheres). From these results, the mean diameter of these macropores is approximately 0.04 micron (400A). Further, since the penetration volume is still increasing with pressure, it appears that more pores still exist within the sample (10,000 psia is the limit of the apparatus).

Inspection of Figure 17 shows that the C-102 sample exhibits the same characteristics as the XAD-2, indicating that the two materials are probably the same. The region between 1000 psia and 4000 psia represents the macropores, which have a mean diameter of about 0.07 micron (700 A), in fairly good agreement with the

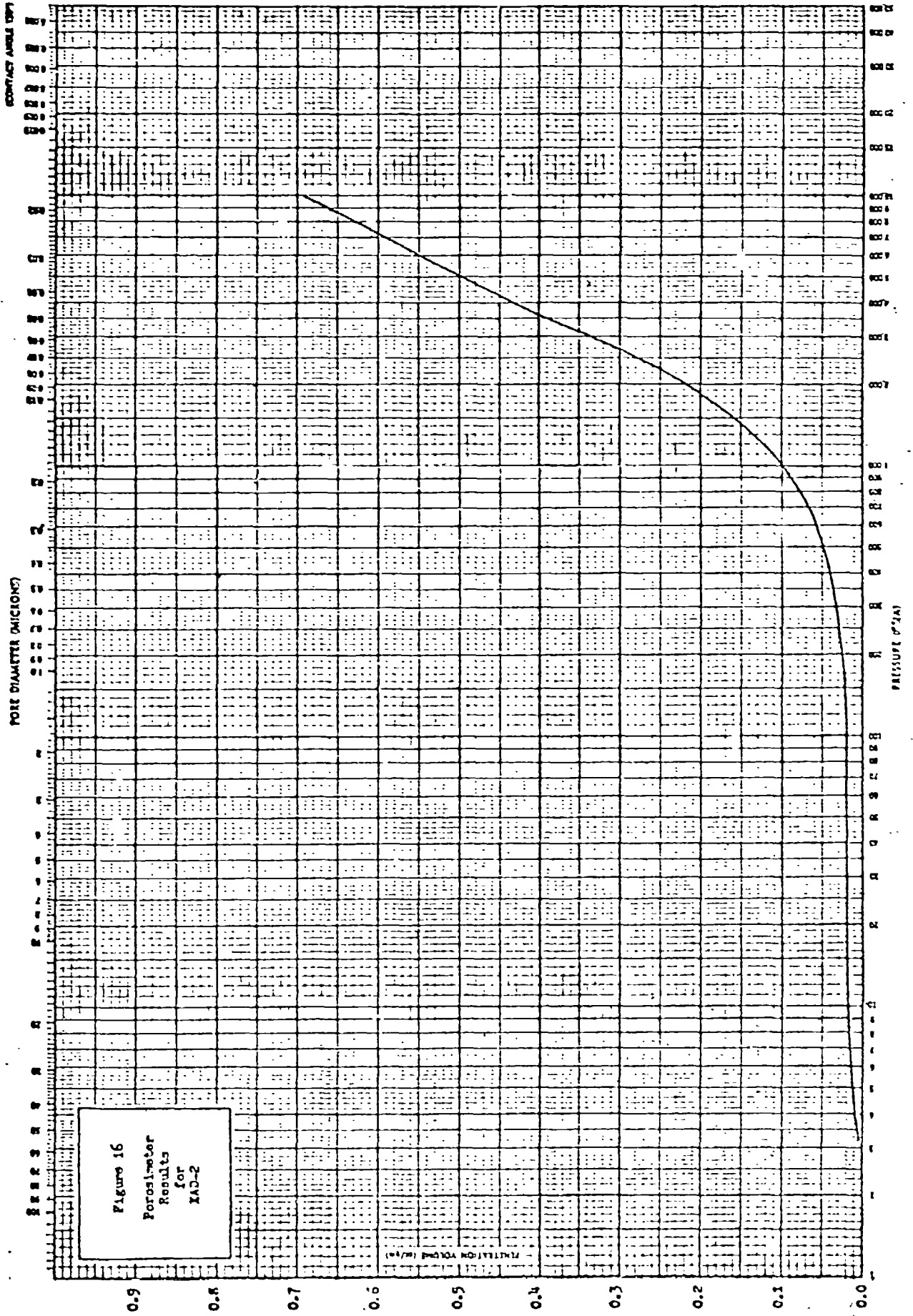
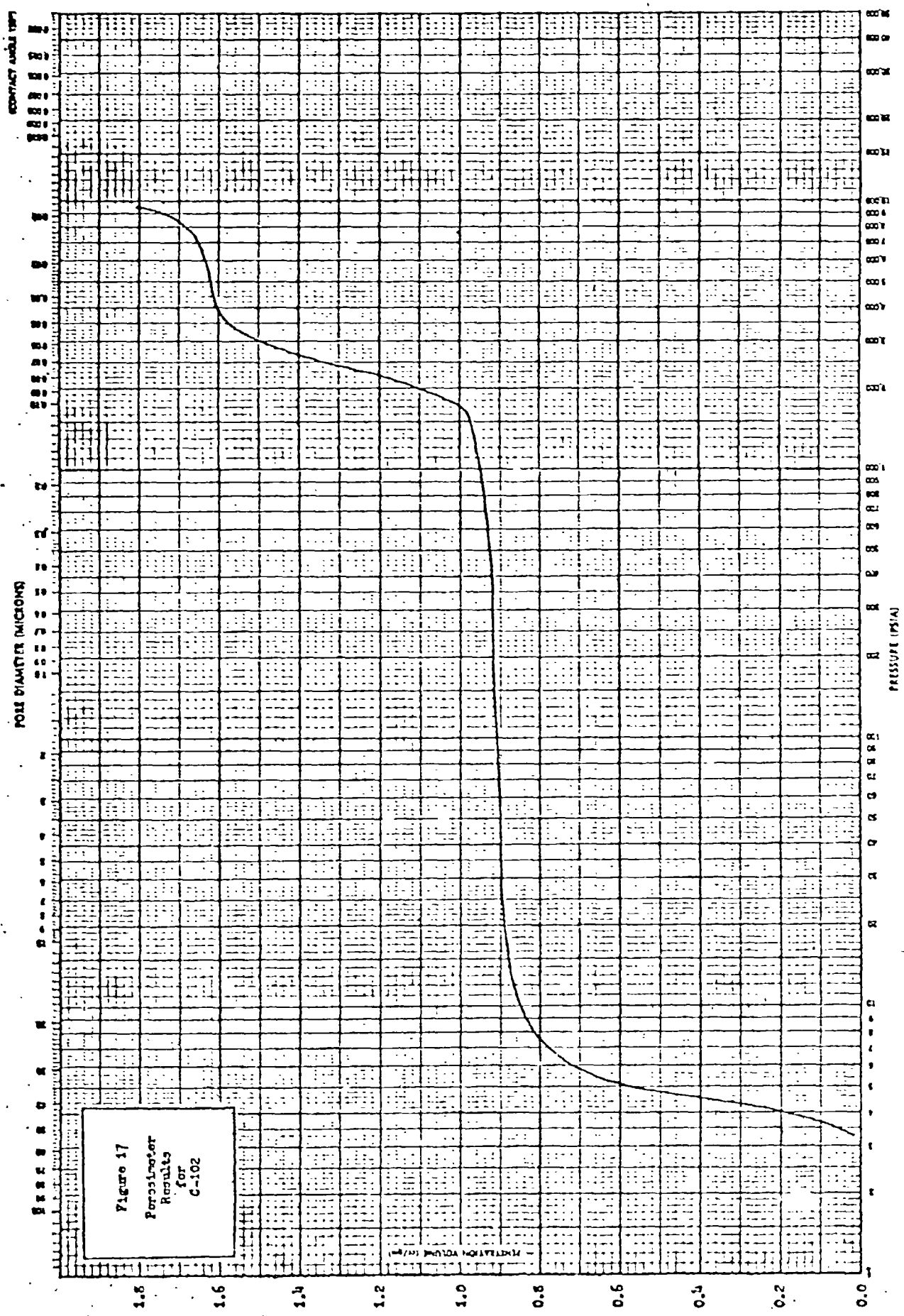


Figure 16
Porosimeter
Results
for
IAD-2



XAD-2 data. The sharp change in slope between 8000 psia and 10,000 psia indicates the presence of more pores of smaller dimension.

Basically, the only difference in the two curves is in the region below 100 psia. This section represents the external void volume for both samples. In the XAD-2, this volume is practically filled even at the lowest pressure (3 psia), while in the C-102 greater pressure is required to fill the voids. This is because the particles of C-102 are much smaller than the XAD-2 (about 1/20 the size), so that the space between C-102 particles is much smaller.

Rohm and Haas reports a mean pore diameter of 90 A. It is possible that this is the mean diameter of the micropores (i.e., the pores of the microspheres). Assuming a contact angle of 130° , a pressure of about 20,000 psia would be needed to fill these pores in the porosimeter. Although this pressure cannot be reached with the apparatus, the presence of these micropores is indicated by the XAD-2 and C-102 data.

Based on the porosimeter results, the void fraction and specific surface area of C-102 were calculated (see Appendix E) to be approximately 0.33 and $72 \text{ m}^2/\text{gm}$ respectively. The value of surface area is much less than the reported value of 300-400 m^2/gm (10). This demonstrates two things: 1) the existence of pores which would be filled at pressures above 10,000 psia; and 2) the large error associated with these results because of the sample holder used. Because of this, the results are considered as a

semi-quantitative representation of the actual properties.

The porosimeter is a valuable tool in determining the properties of the packings. With the proper sample holder, accurate measurements of pore distribution, external void fraction, surface area, and density can be obtained.

G. AUTOMATED DATA PROCESSING

In an attempt to improve consistency in data analysis and to reduce the manual effort in data handling, the automatic data processing scheme shown in Figure 18 was evaluated. This figure also shows the currently used "manual" method of data processing.

In the manual data processing method, the electrical data from the composition detectors at both the column entrance and exit are recorded on a strip chart by means of a visicorder oscillograph. This machine also prints a time scale. Data points are then manually selected from the strip chart at specific time intervals, using an engineer's rule. For data taken in this work, a 0.5 second time interval was used. The discrete data must then be punched on computer cards for final analysis using the computer.

In the proposed automated processing method, the electrical data would be recorded both on magnetic tape by an FM recorder and on the strip chart. This is done for visual certification of the data. The FM recorder would then be taken to a minicomputer and the data read into the machine through an analog-to-digital converter. This produces discrete data points with the specified

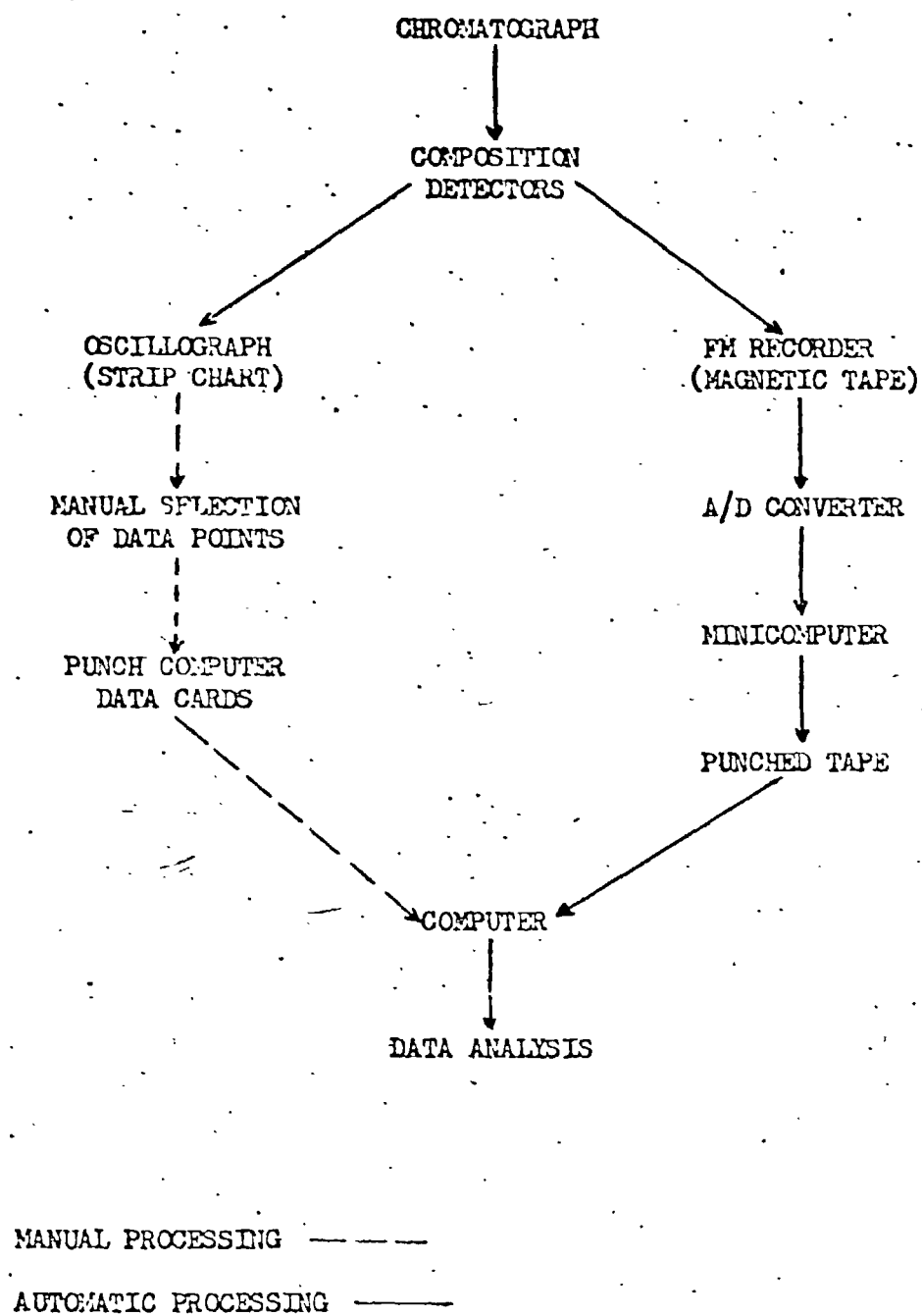
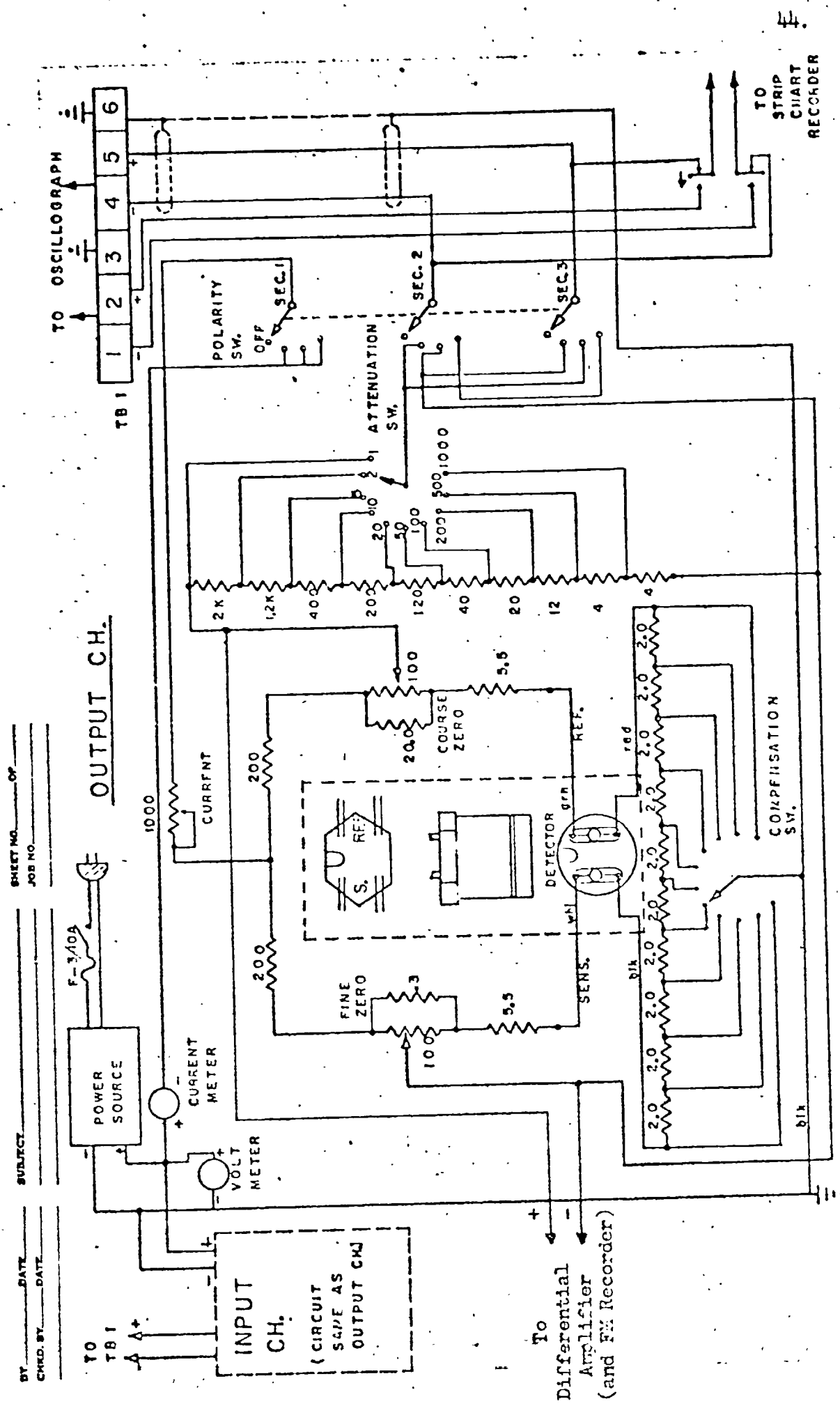


Figure 18 Data Processing

time interval between points. The minicomputer would then produce both a printed listing and a punched tape of the data points. The punched tape would be read directly into the main computer for final data analysis.

The detector control circuit appears in Figure 19, showing the addition of connectors used for the automated system. Since neither side of the Wheatstone bridge is at ground potential, and the FM recorder available (see Appendix F for specifications) records voltages with respect to ground, two differential amplifiers were required. As none were available, an analog computer was used in this capacity for purposes of system evaluation. To develop specifications for the differential amplifiers, measurements of the voltage across the two sides of the bridge were made under various conditions. The results of these tests appear in Table VIII. In order to obtain full output (5 volts) from the FM recorder, differential amplifiers with gains of 1000 are required for samples with dilute components, while gains of 100 will suffice for other samples.

The A/D converter of the minicomputer available for use has a range of -10 v to +10 v and reads voltages at increments of 78 mv. This allows a signal to be broken down into 256 parts at most. Since the output of the FM recorder is only 0 v to 5 v, any data recorded could be resolved into only 64 parts. Resolution of 256 parts could be obtained by biasing the FM recorder output with 2.5 vdc and using a four gain amplifier to provide a signal which ranges from -10 v to +10v.



CARLE DETECTOR CONTROL CIRCUIT - FIG. 19

TABLE VIII
VOLTAGE OUTPUT FROM
WHEATSTONE BRIDGE

C-102 COLUMN

<u>Pulse</u>	<u>Voltage, mv</u>
Input*(maximum)	30.- 45.
Output (maximum)	
Pure Heptane	15.
Dilute Heptane	0.45
50 % Heptane	10.
Pure Pentane	30.
Dilute Pentane	0.35
50 % Pentane	15.

C-1500 COLUMN

<u>Pulse</u>	<u>Voltage, mv</u>
Input*(maximum)	45.
Output*(maximum)	40.

NOISE LEVELS

Output Channel	± 0.02 mv
Input Channel	± 0.01 mv

* approximately the same for all components

A chromatogram on an oscillograph strip chart with full scale deflection (5 inches) can be read with an engineer's rule to the nearest one-hundredth of an inch, giving a maximum resolution of about 500 parts. This is about twice the maximum resolution obtainable from the automatic processing system. It should be noted that the automatic processing will provide consistent data reduction from year to year. However, this consistency can be obtained at the price of: 1) about \$1000-\$1500 for two required differential amplifiers; and 2) less accurate data reduction. It is therefore recommended that the proposed automatic data processing system not be implemented and that attention be directed to obtaining full scale deflection on the oscillograph strip charts.

This can be accomplished by providing variable attenuation in the control circuit (Figure 19). For most samples, an attenuation of one causes the trace to go off scale, while an attenuation of two gives less than full scale deflection. Use of a variable potentiometer in conjunction with the present ten-position potentiometer should provide the capability of obtaining full scale deflection for almost every sample.

Since the manual processing system is time consuming and subject to errors (see Part IV, E), other systems for automatic data processing should be explored. Use of a digital voltmeter with printing capabilities seems feasible, although the cost is high. Such a system should receive more careful attention in future work.

PART V

CONCLUSIONS AND RECOMMENDATIONS

1. Linear superposition offers only a first order representation of actual binary data. The parameter mR_0 is a linear function of component composition.
2. It appears the actual isotherm is non-linear. Studies should be made of the effect of sample size on mR_0 to determine if the isotherm is non-interactive or interactive. Once this is determined, the correct isotherm should be used in the model and changes made to give binary predictions.
3. For pentane and heptane, mR_0 is proportional to $\exp(-E/RT)$ in the temperature range considered. On the porous column, these data are better modeled at higher temperatures.
4. The parameter mR_0 is pressure independent.
5. Heptane data on a non-porous column are well modeled, showing that intraparticle diffusion is probably responsible for observed spreading of heptane data on a porous column.
6. The C-1500 column would not separate the pentane-heptane system at the temperatures considered. Operation of this column at lower temperatures may give separation. Another non-porous column should be considered.
7. The C-102 and XAD-2 appear to be the same material. Each particle is composed of porous macrospheres. The macropores are on the order of 400-700 Å, while the micropores have a mean diameter of 90 Å. A sample holder for powders should be obtained and the porosimeter should be used to determine the packing

characteristics.

8. The proposed automatic data processing system should not be implemented, as the cost involved is not justified.

9. Better resolution of the data can be obtained by obtaining full scale deflection of the trace on the strip chart. This can be done by using variable potentiometers in the control circuit.

10. Many errors are associated with data processing, especially, in manual handling of the data. The value of mR_0 is assumed to be accurate within 20%.

11. Other systems of automatic data processing should be investigated, and the manual system should be evaluated to eliminate sources of error.

PART VI

ACKNOWLEDGEMENT

The author wishes to express his sincere gratitude to Dr. Peter K. Lashmet, who has offered both advice and assistance. Dr. G. Paine of JPL, contract monitor, and Dr. S. Yerazunis, project director for Rensselaer, are also acknowledged for their interest and helpful comments. The author acknowledges financial support from Rensselaer.

PART VII

NOTENCLATURE

E	- activation energy, kcal/gr-mole
F	- fraction of stationary phase volume which is liquid
L	- length of column, cm
m	- adsorption equilibrium constant $= y^*/x_L$
mR_o	- thermodynamic parameter
N_{tOG}	- number of transfer units, dimensionless
Pe	- Peclet number, dimensionless
p	- partial pressure
P	- total pressure
R	- gas constant, 1.987 cal/gr-mole
Re	- Reynolds number, dimensionless
R_o	- ratio of moles of gas to moles of adsorbate in bed
t	- time, sec
T	- temperature, deg K
v	- carrier gas velocity, cm/sec
x_L	- concentration in adsorbent phase
y	- concentration in vapor phase
y^*	- concentration in vapor phase at equilibrium

GREEK LETTERS

β	$= 1 + 1/mR_o$
ϵ	- bed porosity
ρ	- density
σ	- standard deviation
θ	- dimensionless time $= vt/L$

$\theta_{\max,o}$ - dimensionless time of output peak

$\theta_{\max,i}$ - dimensionless time of input peak

SUBSCRIPTS

G - gas phase

L - liquid phase

f - unit impulse response

REFERENCES

1. Sliva, T.F., "Chromatographic Systems Analysis: First Order Model Evaluation", RPI Technical Report MP-1, Rensselaer Polytechnic Institute, Troy, New York, Sept. 1968.
2. Voytus, W.A., "Chromatographic Systems Analysis: Moment Analysis of the Equilibrium Adsorption Model", RPI Technical Report MP-9, Rensselaer Polytechnic Institute, Troy, New York, Aug. 1969.
3. Krum, R.C., "Chromatographic Systems Analysis: Sample Injection Problem", M. Eng. Report, Rensselaer Polytechnic Institute, Troy, New York, June 1969.
4. Taylor, P.N., "Chromatographic Systems Analysis: Second Order Model Development", M. Eng. Report, Rensselaer Polytechnic Institute, Troy, New York, June 1970.
5. Benoit, G.L., "Reduction of Chromatographic Data and Evaluation of a GC Model", RPI Technical Report MP-22, Rensselaer Polytechnic Institute, Troy, New York, June 1971.
6. Keba, P.S., and Woodrow, P.T., "A Comparison of Two Gas Chromatograph Models and Analysis of Binary Data", M. Eng. Report, Rensselaer Polytechnic Institute, Troy, New York, June 1972.
7. Woodrow, P.T., Rensselaer Polytechnic Institute, Troy, New York, (private communication), April 1973.
8. Treybal, R.E., "Mass-Transfer Operations", 2nd ed., McGraw-Hill, New York, 1968, p. 224.
9. Lashmet, P.K., Rensselaer Polytechnic Institute, Troy, New York, (private communication), April 1973.
10. Averill, W., Perkin-Elmer Corp., Norwalk, Conn., (private communication), Jan. 1973.
11. Anon., "Amberlite XAD-2", Technical Bulletin, Ion Exchange Department, Rohm and Haas Company, Philadelphia, Pa., July 1971.

PART IX

APPENDICES

- A. Calculation of Sample Composition in Carrier Gas
- B. Computer Output
- C. Calculations for Moment Analysis
- D. Activation Energy Calculations
- E. Calculations for C-102 Surface Area and Void Fraction
- F. Specifications for FM Recorder

The appendices appear in the reference: Meisch, A.J., "Gas Chromatography: Evaluation of Binary Data and Characterization of Adsorbent Properties," M. Eng. Project Report, Rensselaer Polytechnic Institute, Troy, New York, May 1973. Copies of the material may be obtained from Dr. P. K. Lashmet, Systems Engineering Division, Rensselaer Polytechnic Institute, Troy, New York, 12181.